Available online at www.sciencedirect.com
ScienceDirect
Dyes and Pigments 76 (2008) 133–141
DYES and PIGMENTS
www.elsevier.com/locate/dyepig

Emission based fiber optic pH sensing with Schiff bases bearing dimethylamino groups

Sibel Derinkuyu [a], Kadriye Ertekin [a,*], Ozlem Oter [a], Serpil Denizalti [b], Engin Cetinkaya [b]

[a] University of Dokuz Eylul, Faculty of Arts and Sciences, Department of Chemistry, 35160 Buca, Izmir, Turkey
[b] University of Ege, Faculty of Science, Department of Chemistry, 35100 Bornova, Izmir, Turkey

Received 16 July 2006; received in revised form 21 August 2006; accepted 23 August 2006
Available online 2 October 2006

Abstract

In most of the common designs, pH probes rely on weak acidic dyes whose dissociated and undissociated forms have different absorption or emission maxima. In this work dimethylamino bearing fluorescent Schiff bases **SB-I** and **SB-II** have been characterized and used for pH sensing. Quantum yield and acidity constant (pK_a) calculations of the Schiff bases were performed in the conventional solvents, polyvinyl chloride (PVC) and ethyl cellulose (EC). The immobilized Schiff bases **SB-I** ($pK_a = 4.25$ in PVC) and **SB-II** ($pK_a = 10.68$ in PVC) exhibited absorption and emission based optical response to proton in the pH range of 2.0–7.0 and 8.0–12.0, respectively. Immobilization of the dye effectively enhanced the fluorescence of these materials compared to solution. Responses of the sensor slides were fully reversible within the dynamic working range and the response times were less than 1 min. Relative signal changes of 63% and 95% have been achieved for sensor dyes of **SB-I** and **SB-II** in the PVC matrix, respectively. The cross-sensitivity of the dyes to different metal cations was also investigated. Presence of metal cations in test medium did not restrict the proton sensing ability of the dyes.
© 2006 Elsevier Ltd. All rights reserved.

Keywords: Fiber optic pH sensor; Fluorescent pH indicator; Schiff base

1. Introduction

The ability of chromophore molecules to change their color in response to a pH change has found wide application in research, biotechnology and industry. On the other hand, optical pH sensors are based on pH dependent changes of the optical properties of thin and proton-permeable layers in which a pH indicator has been chemically or physically immobilized. Wolfbeis et al. [1] have used certain coumarins and trisodium salt of 8-hydroxy-1,3,6-pyrenetrisulfonate (HPTS) for measuring near neutral pH values. Zhujun and Seitz [2] prepared a pH sensor by electrostatic immobilization of HPTS on an anion exchange membrane. This sensor allowed the measurements of pH in the range of 6–8. Kawabata et al. [3] immobilized a monolayer of fluorescein directly to the surface of a modified optical fiber. Jordan and Walt [4] developed an energy transfer-based sensor using eosine and phenol red combination for physiological pH ranges. Werner and Wolfbeis presented a pH sensitive membrane for the pH range of 10–13. They covalently immobilized the N8 dye to cellulose on a polyester support and measured the pH dependent absorption of the membrane at 555 nm via optical fibers [5].

Within this time interval, the ''high sensitivity advantage'' of the fluorescent dyes has been the driving force in the development of new fluorescent pH probes or optical sensor devices.

Fluorescein and its diacetate derivatives, carboxyfluorescein and its cell-permeant esters (5-carboxyfluorescein diacetate, acetoxymethyl ester), 5-(and-6)-carboxynaphthofluorescein, 5-(and-6)-carboxy SNARF®-1 (benzenedicarboxylic acid, 2(or 4)-[10-(dimethylamino)-3-oxo-3*H*-benzo[*c*]xanthene-7-yl]-) and

* Corresponding author. Tel.: +90 232 412 8691; fax: +90 232 453 4188/2153.
E-mail addresses: kadriye.ertekin@deu.edu.tr, kadriye.yusuf@superonline.com (K. Ertekin).

0143-7208/$ - see front matter © 2006 Elsevier Ltd. All rights reserved.
doi:10.1016/j.dyepig.2006.08.014

other auxiliary probes for pH measurements were commercialized by Molecular Probes Invitrogen Detection Technologies [6].

Since the fluorescent pH probes are important tools in many areas of biotechnology and biomedical science today, design and development of new fluorescent pH probes are still ongoing. However, further research is required in order to optimise the emission characteristics, lifetimes or photostabilities of the current fluorescence based pH probes.

Here, we declare spectral characterization of two Schiff bases (**SB-I** and **SB-II**) as pH sensing fluorescent molecules for the pH range of 2.0–7.0 and 8.0–12.0, respectively. To our knowledge the **SB-I** and **SB-II** were used for the first time as fluoroionophores in encapsulated form in ethyl cellulose (EC) and plasticized PVC for pH sensing purposes. These dyes have the advantages of long-term photostability, high relative signal change and a large dynamic working range. The response range of the investigated dye pair covers the pH scale from 2.0 to 12.0.

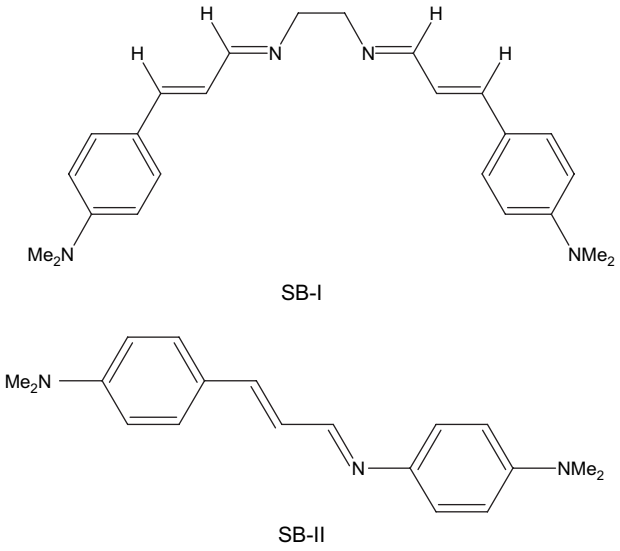

Fig. 1. Chemical structures of the Schiff bases under investigation.

2. Experimental

2.1. Reagents

The polymer membrane components, polyvinyl chloride (PVC) (high molecular weight) and the plasticizer, bis-(2-ethylhexyl)phthalate (DOP), were obtained from Merck and Fluka. Ethyl cellulose (with an ethoxy content of 46%) and potassium tetrakis-(4-chlorophenyl)borate (PTCPB) were from Aldrich. Absolute ethanol (EtOH), tetrahydrofuran (THF), dichloromethane (DCM), and toluene (To) were of analytical grade. Solvents for the spectroscopic studies were used without further purification. Acid solutions were prepared with hydrochloric acid and potassium chloride (for around pH = 2.0), disodium hydrogen phosphate/citric acid (for around pH = 5.0), potassium dihydrogen phosphate/sodium hydroxide (for around pH = 7.0), and boric acid (H_3BO_3)/potassium chloride (KCl) for alkaline pH in carbon dioxide-free water. Millipore water was used throughout the studies. Solutions of metal cations were prepared from respective metal nitrates, sulphates or chlorides and diluted with 5.0×10^{-3} M buffers of demanded pH.

The pH values of the solutions were checked using a digital pH meter (WTW) calibrated with standard buffer solutions of Merck. All the experiments were carried out at room temperature; 25 ± 1 °C. Rose Bengal ($\lambda_{ex} = 525$ nm, quantum yield = 0.11 in alkaline EtOH) was used as reference for fluorescence quantum yield calculations of the **SB-I** and **SB-II**.

2.2. Synthesis of the Schiff bases

The Schiff bases **SB-I** – N^1,N^2-bis{(*E*,2*E*)-3-[4-dimethylamino)phenyl]-2-propenylidene}-1,2-ethanediamine – and **SB-II** – N^1{(*E*,2*E*)-3-[4-dimethylamino)phenyl]-2-propenylidene}-N^4,N^4-dimethyl-1,4-benzene-diamine – were synthesized in our laboratories similar to the literature procedure [7]. Schematic structures of the employed molecules **SB-I** and **SB-II** are shown in Fig. 1.

^{1}H NMR of **SB-I**: ($CDCl_3$, 400 MHz, δ): 2.98 (s, 12H, NCH_3); 3.76 (s, 4H, NCH_2); 6.6; 7.3 (d, $J = 2.3$ Hz, 8H, $Me_2N-C_6H_4$); 6.7 (dd, $J = 4$ Hz, 2H, $Me_2NC_6H_4-CH{=}CH$); 6.8 (d, $J = 4$ Hz, 2H, $Me_2NC_6H_4-CH{=}CH$); 7.96 (d, $J = 2.1$ Hz, 2H, $CH{=}N$). ^{13}C NMR of **SB-I** ($CDCl_3$, 400 MHz, δ): 164.55 ($CH{=}N$); 151.06; 142.25; 128.78; 112.32 (Caren); 124.44; 124.10 (C=C); 62.10 (NCH_2); 40.45 (NCH_3). m.p. of **SB-I**: 195–198 °C.

^{1}H NMR of **SDC**: ($CDCl_3$, 400 MHz, δ): 2.96; 3.0 (s, 12H, NCH_3); 6.7 (m, 4H, $Me_2NC_6H_4C$; $Me_2NC_6H_4N$); 6.95 (m, 2H, $Me_2NC_6H_4-CH{=}CH$); 7.16 (d, $J = 2.2$ Hz, 2H, $Me_2NC_6H_4N$); 7.38 (d, $J = 2.2$ Hz, $Me_2NC_6H_4C$); 8.25 (d, $J = 2$ Hz, $CH{=}N$). ^{13}C NMR of **SDC**: ($CDCl_3$, 400 MHz, δ): 157.97 ($CH{=}N$); 151.17; 149.36; 128.97; 124.94; 124.65; 122.20; 113.24; 112.36 (Caren); 142.78 ($C{=}C$); 41.01; 40.45 (NCH_3). m.p. of **SB-II**; 238–240 °C.

2.3. Instrumentation

Absorption spectra were recorded using a Shimadzu 1601 UV–vis spectrophotometer. Steady-state fluorescence emission and excitation spectra were measured using Varian Cary Eclipse Spectrofluorometer with a Xenon flash lamp as the light source.

pH measurements were carried out with fiber optic probe (2 m long) and solid sample tip accessories constructed on the spectrofluorometer. For instrumental control, data acquisition and processing the software package of the spectrofluorometer was used.

The tip of the bifurcated fiber optic probe was interfaced with a sensing film in a buffer containing homemade 300 μL flow cell (See Fig. 2). The flow cell was equipped with a four channel Ismatec Reglo Analog peristaltic pump. Flow rate of the peristaltic pump was kept at 2.2 mL min^{-1}. Analyte solutions or buffers were transported by an Ismatec peristaltic pump via tygon tubing of 2.06 mm i.d.

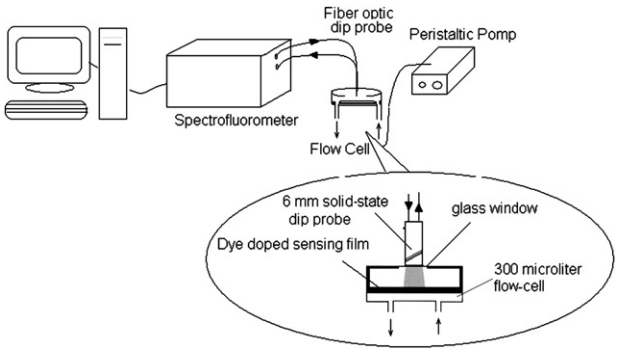

Fig. 2. Instrumental setup used for dye-doped thin film evaluation.

3. Results and discussion

3.1. Spectral characterization studies in solvents

Absorption, excitation, and corrected emission spectra of the **SB-I** and **SB-II** were recorded in the solvents of EtOH, DCM, THF and toluene/ethanol mixture. Spectral data of the reference standard Rose Bengal were acquired in EtOH and in solid matrices of PVC and EC, respectively. In all the employed solvents the **SB-I** and **SB-II** were excited at around 400 nm and the emission spectra were recorded. The emission spectra were corrected using commercially available silica ground of Cary Eclipse. The UV–vis spectroscopy related data (absorption maxima, $\lambda_{abs,}$ and molar extinction coefficient, ε) are shown in Table 1.

The **SB-I** and **SB-II** exhibited very efficient absorbance and high molar extinction coefficients around 400 nm and 500 nm in all the employed solvents and solid matrices, respectively. In agreement with literature, molar extinction coefficients (ε_{max}) of **SB-I** and **SB-II** in polymer matrices were increased about 3500-fold, with respect to (ε_{max}) of **SB-I** and **SB-II** in solutions [8]. The $\varepsilon^{EC}_{max1}/\varepsilon^{DCM}_{max1}$ ratios were 3551 and 3388 for **SB-I** and **SB-II**, respectively. These data can be taken as proofs that **SB-I** and **SB-II** molecules absorb better in immobilized EC or PVC matrices.

Table 1
UV–vis spectra related data of **SB-I** and **SB-II** in the solvents of EtOH, DCM, THF and toluene/ethanol mixture (80:20) and in solid matrices of PVC and EC

Compound	Solvents/ matrix	n (refractive index)	λ^1_{abs}	λ^2_{abs}	$\varepsilon_{max}(\lambda^1_{abs})$	$\varepsilon_{max}(\lambda^2_{abs})$
SB-I	EtOH	1.3590	370	472	58 900	17 500
SB-I	DCM	1.4241	360	–	53 500	–
SB-I	THF	1.4070	–	–	–	–
SB-I	To:EtOH	1.4694	372	–	54 200	–
SB-I	PVC	1.5200	379	495	1.2×10^8	1.3×10^8
SB-I	EC	1.4790	390	490	1.9×10^8	2.1×10^8
SB-II	EtOH	1.3590	–	–	–	–
SB-II	DCM	1.4241	400	–	30 700	–
SB-II	THF	1.4070	405	–	45 500	–
SB-II	To:EtOH	1.4694	416	–	38 100	–
SB-II	PVC	1.5200	426	563	9.1×10^7	2.9×10^8
SB-II	EC	1.4790	413	560	1.04×10^8	8.2×10^7

3.2. Cocktail preparation protocols and spectral evaluation

The optode membranes were prepared to contain 120 mg of PVC, 240 mg of plasticizer, 1.0 mg of **SB-I** or **SB-II** (2.5 mmol dye/kg polymer), 1.49 mg of potassium tetrakis-(4-chlorophenyl)borate and 1.5 mL of THF. The prepared cocktails contained 33% PVC and 66% plasticizer by weight which is quite common [9–11,13].

The resulting cocktails were spread onto a 125 μm polyester support (Mylar™ type) in order to obtain the sensing films. The polyester support was optically fully transparent, ion impermeable and exhibited good adhesion to PVC. Film thickness of the sensing slides was measured with a Tencor Alpha Step 500 Prophylometer and found to be 5.18 μm. This result was an average of 10 measurements and exhibited a standard deviation of ±0.071. Each sensing film was cut to 1.2×3.0 cm size and fixed diagonally into the sample cuvette and the excitation and fluorescence emission spectra were recorded for spectral characterization. The Schiff bases, **SB-I** and **SB-II**, were excited at 510/500 and 570/595 nm in PVC and EC, respectively (see Fig. 3 and Table 2).

The sensor films of 30 mm diameter were cut and placed into the buffer containing 300 μL black-Teflon flow cell and interfaced with the fiber tip (6 mm diameter). The contact between the sensor membrane and the buffer provides a constant

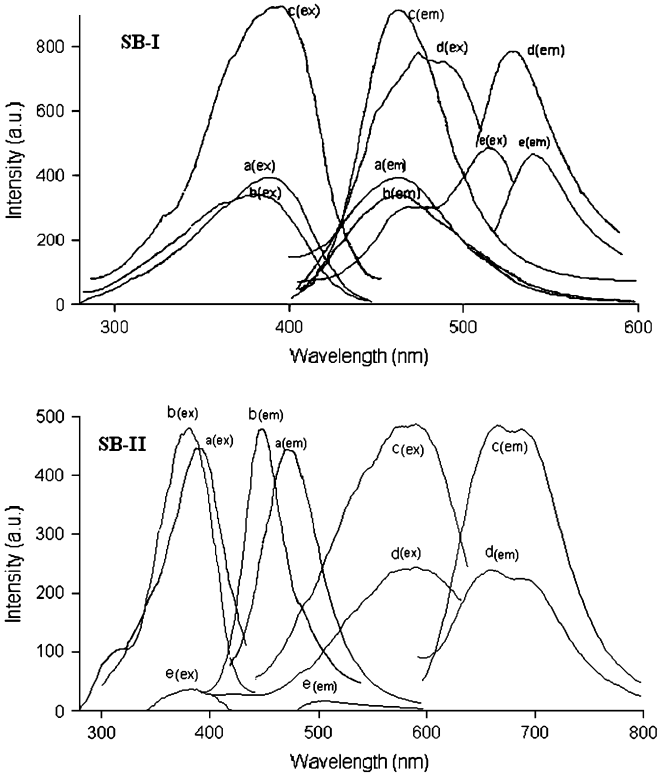

Fig. 3. Excitation and corrected emission spectra of the **SB-I** and **SB-II** dyes (10^{-6} M dye or 2 mM dye/kg polymer). **SB-I**: (a) Toluene/ethanol (80:20), (b) EtOH, (c) DCM, (d) EC, (e) PVC. **SB-II**: (a) Toluene/ethanol (80:20), (b) DCM, (c) EC, (d) PVC, (e) THF.

Table 2
Spectral characterization of **SB-I** and **SB-II** dyes

Compound	Solvent or matrix	λ_{ex}^{em} (excitation wavelength for emission)	λ_{ex}^{ex} (emission wavelength for excitation)	λ_{max}^{em}	λ_{max}^{ex}	$\Delta\lambda_{ST}$ (Stoke's shift)	(ϕ_F) (quantum yield)
SB-I	EtOH	385	464	464	385	79	0.0179 in DCM
SB-I	DCM	390	453	453	390	63	
SB-I	THF	–	–	–	–	–	
SB-I	To:EtOH	390	461	461	390	71	
SB-I	PVC	510	540	540	510	30	0.2320
SB-I	EC	500	535	535	500	35	0.0880
SB-II	EtOH	–	–	–	–	–	0.0029 In To:EtOH
SB-II	DCM	386	460	460	386	74	
SB-II	THF	420	479	479	420	59	
SB-II	To:EtOH	390	474	474	390	84	
SB-II	PVC	570	665	665	570	95	0.0130
SB-II	EC	595	656	656	595	61	0.0078

λ_{ex}^{em}: excitation wavelength for emission in nm; λ_{ex}^{ex}: excitation wavelength for excitation in nm; λ_{max}^{em}: maximum emission wavelength in nm; λ_{max}^{ex}: maximum excitation wavelength in nm; $\Delta\lambda_{ST}$: Stoke's shift and ϕ_F: quantum yield.

fluorescence signal. During fiber optic measurements the fluorescence intensity was monitored and recorded versus time. pH determinations were carried out pumping buffer solutions of desired pH. Each buffer solution was pumped for 2 min at a flow rate of 2.2 mL min^{-1}.

3.3. Fluorescence quantum yield calculations and interpretation of emission spectra

Fluorescence quantum yield values (ϕ_F) of the **SB-I** and **SB-II** were calculated employing the comparative William's method [12], which involves the use of well-characterized standards with known ϕ_F values. For this purpose, the UV–vis absorbance and corrected emission spectra of different concentrations of reference standard (Rose Bengal) and **SB-I** or **SB-II** were recorded.

The integrated fluorescence intensities were plotted versus absorbance for the reference standard and the Schiff bases, **SB-I/SB-II**, in the PVC and EC matrices. The gradients of the plots were proportional to the quantity of the quantum yield of the studied molecules.

Quantum yield (ϕ_F) values were calculated according to the following equation where ST and X denote standard and sample, respectively, Grad is the gradient from the plot and n is the refractive index of the solvent or polymer matrix material [12].

$$\phi_F = \phi_{ST}\left(\frac{Grad_X}{Grad_{ST}}\right)\left(\frac{n_x^2}{n_{ST}^2}\right)$$

The **SB-I** displayed enhanced fluorescence emission quantum yield, $\phi_F = 0.2320$ and longer excitation wavelength $\lambda_{ex}^{em} = 510$ nm in immobilized PVC compared to $\phi_F = 0.0880$ and $\lambda_{ex}^{em} = 500$ nm in EC (see Table 2). Stoke's shift decreased to 30 nm in plasticized PVC film with respect to Stoke's shift of 35 nm in EC matrix. Red shift of absorption and emission of **SB-I** and **SB-II** may be related to enhanced conjugation in immobilized polymer phase by hindrance of vibrational rotational motions. Decrease of Stoke's shifts ($\Delta\lambda_{ST}$), in the order of EtOH, To:EtOH (80:20), DCM solutions and PVC film – 79, 71, 63 and 30 nm, respectively – is evidence of restricted vibrational rotational motions.

Differences in the Stoke's shifts of the dyes in EtOH and DCM can be attributed to differences in solvent polarities, but the decrease of Stoke's shift in polymer film arises from lowered difference of equilibrium geometries between ground and excited states in immobilized phase with respect to solutions.

In agreement with literature [8], fluorescence quantum yield (ϕ_F) of **SB-I** and **SB-II** in PVC, increased about 13-fold and 4.5-fold, with respect to ϕ_F of **SB-I** and **SB-II** in solutions which can be concluded as proofs that both the Schiff bases **SB-I** and **SB-II** fluoresce better in immobilized PVC matrix.

3.4. Acid–base behavior of the Schiff bases

Protonation–deprotonation equilibria of the fluorescent Schiff bases investigated are shown in Fig. 4. Both the employed Schiff bases contain available active centers for proton attacks and are appropriate for use as pH probes. The Schiff bases display intramolecular charge transfer in the excited state since the *N*,*N*-dimethylamino moiety is an electron donating group compared to the nitrogen atoms N^1 and N^2. Therefore, acid–base behavior of the symmetric Schiff base N^1,N^2-bis{(*E*,2*E*)-3-[4-dimethylamino)phenyl]-2-propenylidene}-1,2-ethanediamine can be attributed to the successive protonation of the nitrogen atoms N^1 and N^2. Protonation of the excited states of the Schiff bases results in an increase in the luminescence intensity in low pH solutions. In a similar way, the acid–base chemistry of the non-symmetric Schiff base, N^1{(*E*,2*E*)-3-[4-dimethylamino)-phenyl]-2-propenylidene}-N^4,N^4-dimethyl-1,4-benzene-diamine (**SB-II**), is assigned to the stepwise protonation of the N^1 and N^4 moieties. In both cases, at low pHs, protons are reversibly extracted into the PVC or EC membrane by the lipophilic anionic additive as can be seen while comparing the work of Wolfbeis et al. [13].

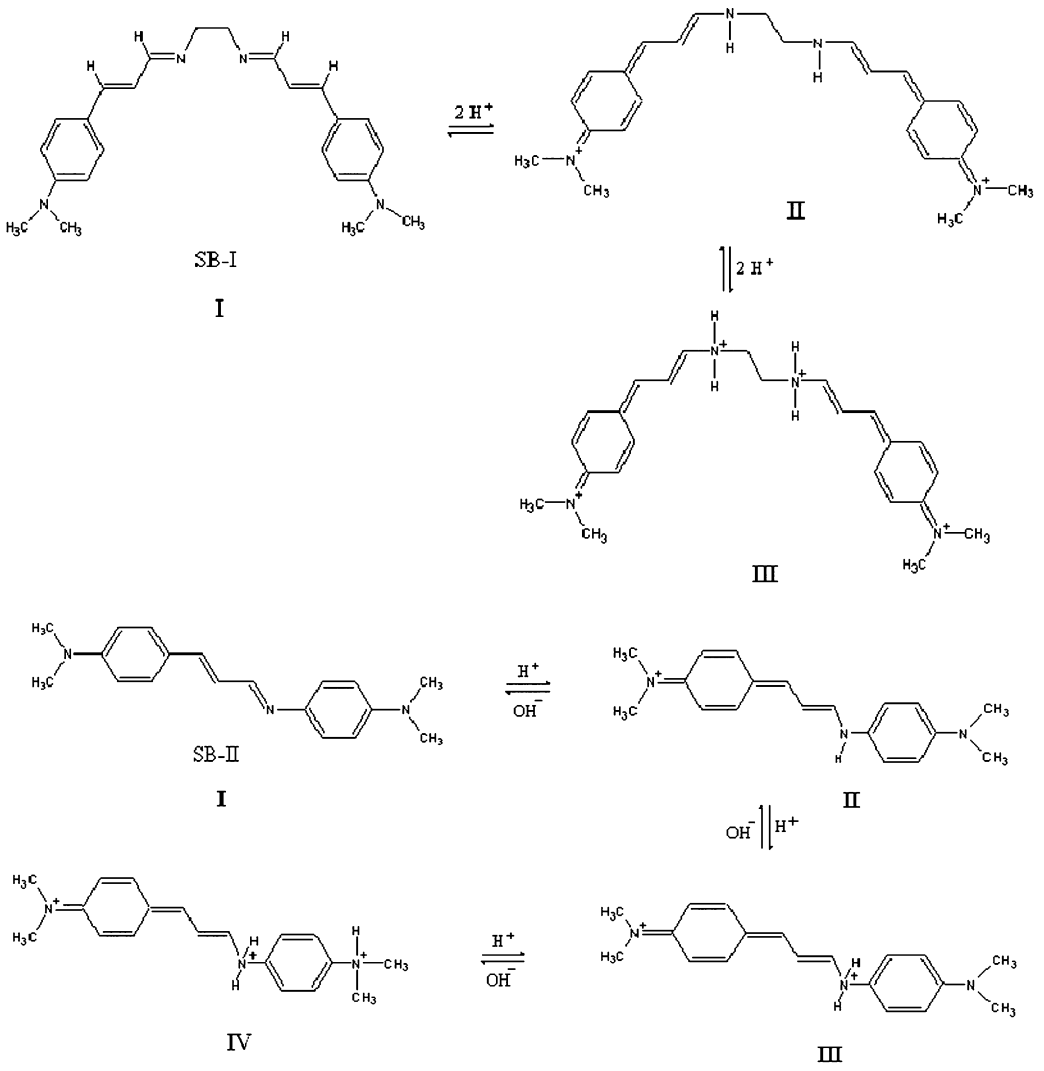

Fig. 4. Protonation–deprotonation equilibria of Schiff bases;| **SB-I**: N^1,N^2-bis{(*E*,2*E*)-3-[4-dimethylamino)phenyl]-2-propenylidene}-1,2-ethanediamine and **SB-II**: N^1{(*E*,2*E*)-3-[4-dimethylamino)phenyl]-2-propenylidene}-N^4,N^4-dimethyl-1,4-benzene-diamine.

After the stepwise protonation of the acid-sensitive moieties, the color turns from pale red to orange and from yellow to dark purple in the **SB-I** and **SB-II**, respectively.

3.5. Photostability of CPIPA and NPIPA

Unlike fluorescent materials such as fluorescein and rhodamine, which are rapidly bleached, the Schiff bases possess great stability towards degradation by visible irradiation both in solution and in plasticized polymer matrices. The photostabilities of the Schiff bases were tested and evaluated in $CHCl_3$ and THF and in solid matrices of PVC and EC under Xenon-arc lamp and solar radiation. Photostability tests of SB derivatives were carried out with the steady-state spectrofluorometer in the mode of "Time Based Measurements". The **SB-I** and **SB-II** were excited at 500 and 595 nm, respectively, and the data were acquired at their maximum emission wavelengths during 2 h of monitoring. In all the employed media the Schiff bases exhibited excellent short-term photostability. Fig. 5 reveals short-term stability performance of the EC doped **SB-I** and **SB-II** in immobilized phase.

The long-term photostabilities of both derivatives in PVC and EC were tested after eight months and found to be nearly the same with an intensity loss of only 2%.

3.6. pK_a calculations of *SB-I* and *SB-II* in EtOH

The knowledge of dissociation constant (pK_a) of **SB-I** and **SB-II** is of fundamental importance in order to provide information on chemical reactivity range of the indicator dyes. In order to evaluate the availability of **SB-I** and **SB-II** molecules for sensing purposes, determination of the acidity constants has been performed in different media. The sensor dyes irreversibly responded to H^+ ions in the solution phase. Fig. 6

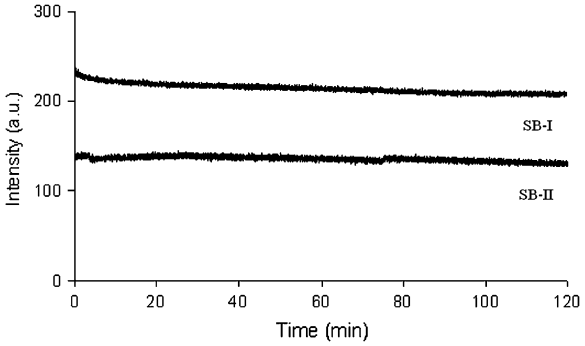

Fig. 5. Photostability test results of **SB-I** and **SB-II** in EC matrix after exposure to Xenon-arc lamp at 500 nm for 2 h of monitoring.

reveals the emission based response of the **SB-I** and **SB-II** to H^+ ions in EtOH. In both the Schiff bases, approximately 20 nm of spectral shift was observed after exposure to H^+ ions (see Fig. 6). The effective p*K*a values were determined to be $Ka_1 = 6.80$ and $Ka_2 = 8.05$ for **SB-I**, and, $Ka_1 = 4.62$ for **SB-II** in EtOH.

3.7. pK_a calculations of *SB-I* and *SB-II* in PVC matrix

The immobilized Schiff bases reversibly responded to H^+ ions in PVC. The relative signal change of absorption spectra of the **SB-I** and **SB-II** was monitored after addition of certain concentrations of buffered acid solutions at different pH ranges. The immobilized **SB-II** exhibited the best response to different concentrations of acid solutions between pH 8.0 and 12.0 in the direction of a decrease in signal intensity at 563 nm in absorption spectrum. Due to the presence of the isobestic point at 483 nm the **SB-II** dye allows absorption-based ratiometric measurements in plasticized polymer PVC and EC matrices. However, the isobestic point becomes unclear in case of **SB-I** (see Fig. 7). The **SB-I** works in the pH range of pH = 2.0–7.0. Upon exposure to the solutions between pH 2.0 and 7.0, the **SB-I** dye exhibited a 79% relative signal change in the direction of decrease in absorbance intensity at 379 nm. The absorption-based relative signal change of **SB-II** in the pH range of 8.0–12.0 was 96% (see Fig. 7).

Figs. 8 and 9 show emission based spectral response of PVC doped **SB-I** and **SB-II** to pH in the pH range of 2.0–7.0 and 8.0–12.5, respectively. The immobilized **SB-I** and **SB-II** exhibited a decrease in signal intensity after exposure to different concentrations of acid solutions between pH = 2.0–7.0 and pH = 8.0–12.5 in signal intensity at 540 and 665 nm, respectively.

For both dyes, the plots of the absorption or emission based intensities versus pH exhibited "S" shaped calibration graphs with one inflection point. p*K*a values were calculated via equation

$$pK_a = pH + \log[(I_x - I_b)/(I_a - I_x)] \quad (1)$$

where I_a and I_b are the signal intensities of the dyes in their acid and conjugate base form, respectively [14]. The emission based pK_a values were found as 4.25 and 10.68 for **SB-I** and **SB-II** in PVC, respectively.

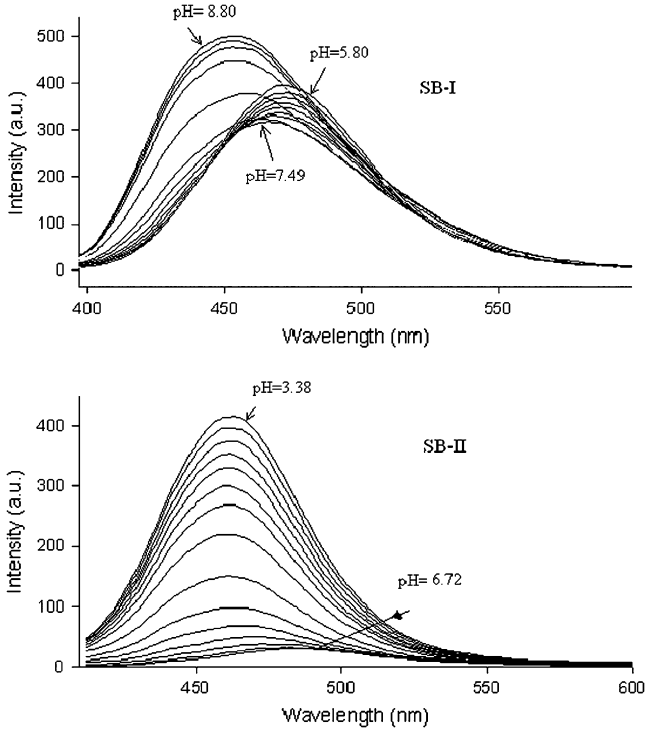

Fig. 6. pH dependent emission spectra of **SB-I** and **SB-II** in EtOH. **SB-I**: Intermediate spectra between pH 8.80 and 7.49 (pH = 8.75, 8.69, 8.30, 8.05, 7.88, 7.77, 7.65) at 453 nm and between pH 7.49 and 5.80 (pH = 7.40, 7.21, 6.95, 6.80, 6.37, 6.14) at 473 nm. **SB-II**: Intermediate spectra between pH 6.72 and 3.38 (pH = 6.22, 5.98, 5.78, 5.54, 5.25, 4.97, 4.58, 4.33, 4.11, 3.86, 3.69, 3.58) and accompanying spectral shift from 485 to 461 nm.

3.8. pK_a calculations of *SB-I* and *SB-II* in EC matrix

Dissociation constants (pK_a) of **SB-I** and **SB-II** in ethyl cellulose matrix were calculated from the excitation/emission based measurements according to Eq. (1). EC doped **SB-I** and **SB-II** exhibited a parallel decrease both in emission and excitation intensity after exposure to different concentrations of acid solutions in the pH range of pH = 2.0–7.0 and pH = 8.0–12.0, respectively. In EC doped films the pK_a values of **SB-I** and **SB-II** were found to be 3.87 and 9.68, respectively. Fig. 10(I) and 10(II) show pH induced emission/excitation based spectral response of the EC doped **SB-I** and **SB-II** in the pH range of 2.0–7.0 and 8.0–12.0, respectively.

Depending on the matrix, the p*K*a values of **SB-I** and **SB-II** exhibited differences. In EtOH, two apparent p*K*a values were obtained for **SB-I** ($Ka_1 = 6.80$ and $Ka_2 = 8.05$), whereas, only one p*K*a value was observed for **SB-I** in solid matrices of PVC and EC which are 4.25 and 3.87, respectively. The differences in p*K*a can be attributed to the protonation difficulty of symmetric **SB-I** in PVC. Similar matrix dependent large differences in the apparent p*K*a values were reported earlier [13]. The **SB-II** exhibited the p*K*a values of 4.62, 10.68 and 9.68 in EtOH, PVC and EC, respectively. p*K*a value of non-symmetric **SB-II** is lower by approximately 6 p*K*a units in EtOH than that in PVC or EC. This can be attributed to the polarity differences of the

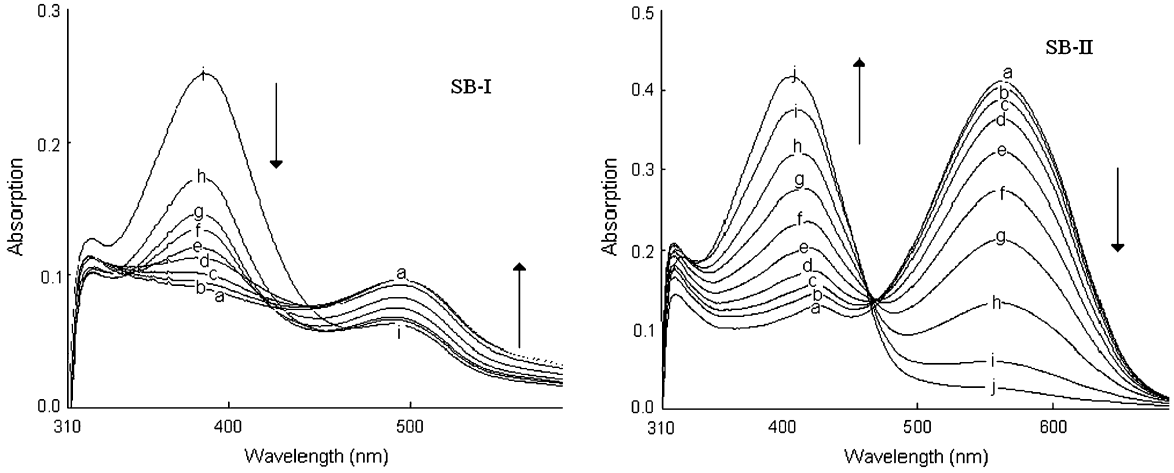

Fig. 7. Absorption spectra of **SB-I** and **SB-II** in PVC after addition of acid solutions in the pH range of 2.0–7.0 and 8.0–12.5. **I.** pH: (a) 2.0, (b) 3.0, (c) 3.5, (d) 4.0, (e) 4.5, (f) 5.0, (g) 5.5, (h) 6.0, (i) 7.0. **II.** pH: (a) 8.0, (b) 8.5, (c) 9.0,(d) 9.5, (e)10.0, (f)10.5, (g) 11.0, (h) 11.5, (i) 12.0, (j) 12.5.

matrices as well as the structure of the dye. The OH groups of ethyl cellulose probably interact with the immobilized Schiff bases making weak hydrogen bonds or via the acid-sensitive moieties of the dye complexes. Interactions between support material and the dye can be beneficial to sensor performance giving stability.

3.9. Dynamic working range and sensor response

The sensor slides were found to give reproducible results on absorption and fluorescence emission measurements when pH was varied within the dynamic working range. The response of **SB-I** and **SB-II** to protons was investigated in buffered solutions. Fig. 11 shows the relative signal change, and reversibility performance of the PVC doped **SB-I** and **SB-II**. Relative signal changes of 63% and 95% have been achieved for sensor dyes of **SB-I** and **SB-II** in the PVC matrix, respectively. Regeneration was accomplished with concentrated buffer solutions at opposite pHs. The Schiff bases were found to reach 90% of the signal intensity (τ_{90}) between 80 s and 3.2 min. Since the ion binding process is faster than that of unbinding,

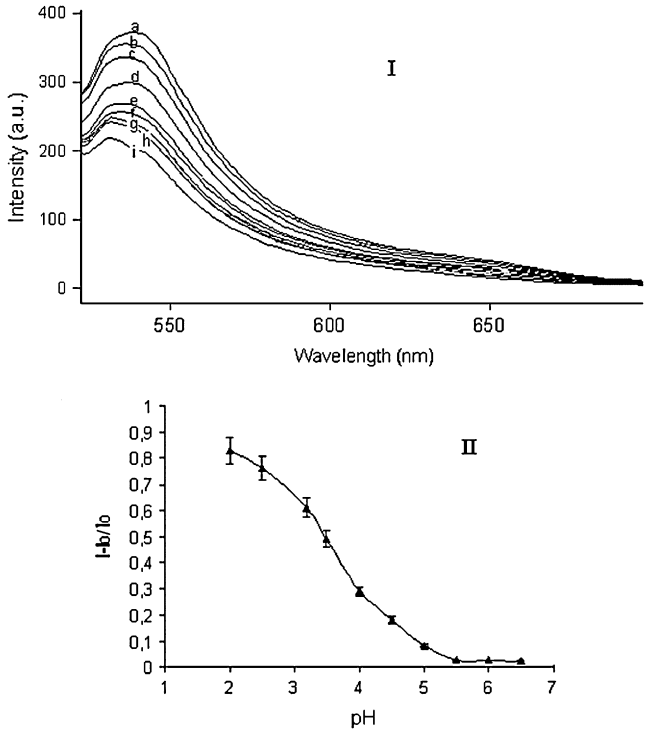

Fig. 8. **I**: pH induced emission based spectral response of the PVC doped **SB-I** in the pH range of 2.0–7.0. pH: (a) 2.0, (b) 2.5, (c) 3.0, (d) 3.5, (e) 4.0, (f) 4.5, (g) 5.0, 5.5, (h) 6.0, 6.5, (i) 7.0. **II**: Emission based sigmoidal response of **SB-I** to pH.

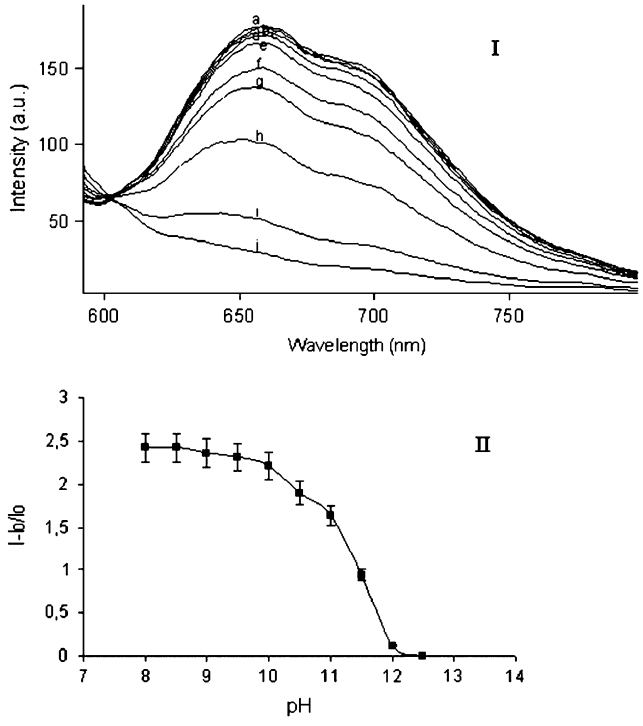

Fig. 9. **I**: pH induced emission based spectral response of the PVC doped **SB-II** in the pH range of 8.0–12.5. pH: (a) 8.0, (b) 8.5, (c) 9.0, (d) 9.5, (e) 10.0, (f) 10.5, (g) 11.0, (h) 11.5, (i) 12.0, (j) 12.5 in boric acid buffered solutions. **II**: Emission based sigmoidal response of **SB-II** to pH in the pH range of 8.0–12.5.

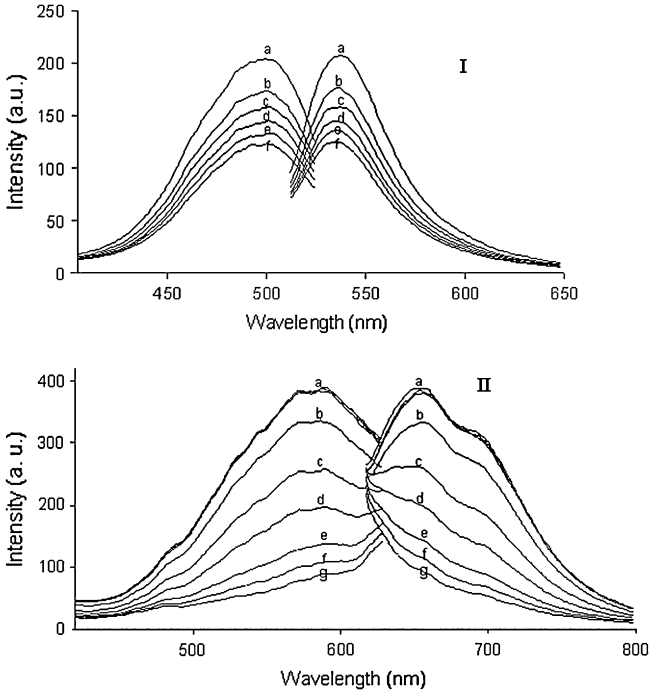

Fig. 10. pH induced emission based spectral response of the EC doped **SB-I** and **SB-II** in the pH range of 2.0–7.0 and 8.0–12.0. **II**. pH: (a) 2.0, (b) 3.0 (c) 4.0, (d) 5.0, (e) 6.0, (f) 7.0 buffered solutions. **II**. pH: (a) 8.0, 8.5, 9.0, (b) 9.5, (c) 10.0, (d) 10.5 (e) 11.0 (f) 11.5, (g) 12.0.

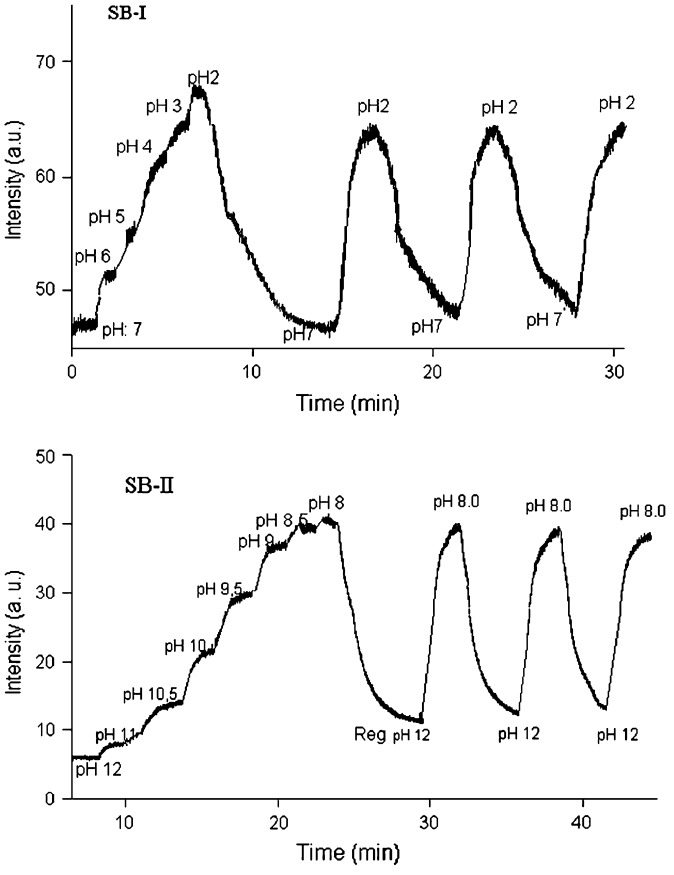

Fig. 11. Response curve and regeneration performance of PVC doped **SB-I** and **SB-II**. Data were acquired with fiber optic probe which is in contact with flow system.

the regeneration time for all sensors was found to be approximately 15–20 min in buffer solutions. However, the upper limit of response time can be improved. In our case, film thickness is approximately 5 μm, which can be reduced and shorter response times can be reached.

3.10. Cross-sensitivity to metal cations

The cross-sensitivity of the Schiff bases used in this study to Na^+, K^+, and many polyvalent metal ions was investigated by exposure to 10^{-3} M solutions of Zn^{2+}, Hg^+, Sn^{2+} Ca^{2+}, Bi^{2+}, Na^+, Ni^{2+}, Co^{2+}, Cu^{2+}, Pb^{2+}, Al^{3+}, Cr^{3+}, Mn^{2+}, K^+, Fe^{2+} and Fe^{3+}. Fig. 12 reveals intensity based response of **SB-I** and **SB-II** to the metal cations in phosphate buffered solutions at pH 7.0.

Presence of H^+ in an ion-free solution enhances the fluorescence intensity of the immobilized **SB-I** without a spectral shift. The most notable source of interference to the pH sensitivity of the **SB-I** is the quenching of the excited state by the cations of Zn^{2+}, Co^{2+}, Cr^{3+}, Mn^{2+}, Fe^{2+} and Fe^{3+} at neutral pH. It should be noted that, response of the **SB-I** to the analyte is in the opposite direction to that of the responses of the interferens. Spectroscopic responses to metal ions are dependent on many factors, including pH, temperature, viscosity, and the presence of other ions.

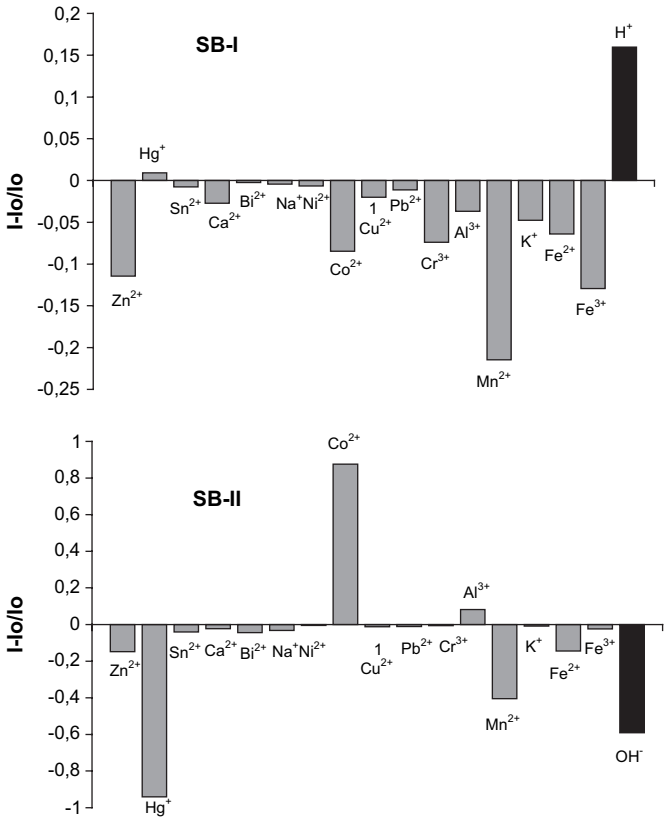

Fig. 12. Metal-ion response test for **SB-I** and **SB-II**. Results are plotted as relative fluorescence changes, $(I - I_o)/I_o$, where I is the fluorescence intensity of the sensor membrane after exposure to ion-containing solutions and I_o is the fluorescence intensity of the sensor slide in ion-free buffer solution.

The immobilized **SB-II** exhibits a pH dependent decrease in fluorescence signal intensity after exposure to alkaline solutions. In this case the potential interferents are Co^{2+}, Mn^{2+} and Hg^{+}.

It is possible to measure pH with these optodes, but only if cations of Zn^{2+}, Co^{2+}, Cr^{3+}, Mn^{2+}, Fe^{2+}, Fe^{3+} and Hg^{+} in the analyte solution have constant activity.

4. Conclusion

We demonstrate that the fluorescent Schiff bases **SB-I** and **Sb-II** can be used for reversible fiber optic pH sensing when doped into the plasticized PVC and EC matrices. In the present absorption and emission based studies, the dynamic working range of the Schiff bases has been determined as pH = 2.0–7.0 and 8.0–12.5 for **SB-I** and **SB-II**, respectively. Zn^{2+}, Co^{2+}, Cr^{3+}, Mn^{2+}, Fe^{2+}, Fe^{3+} and Hg^{+} ions should be considered as possible interferents, and, in the presence of these ions their activities should be kept constant.

The compatibility of the employed Schiff bases with the solid-state optical components (in particular LED's emitting in the wavelength range of 510–590 nm and fiber optics) can be useful in the construction of inexpensive and field available instrumentation. Our work along these lines but on different matrix is in progress.

Acknowledgements

Fund for this research was provided by the TUBITAK (Kariyer Project—104M268) and Scientific Research Funds of Dokuz Eylul University (Project No: 2005 KB Fen 18).

References

[1] Wolfbeis OS, Fürlinger E, Kroneis H, Marsoner H, Fresenius Z. A study on fluorescent indicators for measuring near neutral (''physiological'') pH-values. Analytical Chemistry 1983;314:119–24.
[2] Zhujun Z, Seitz WR. A carbon dioxide sensor based on fluorescence. Analytica Chimica Acta 1984;160:305–9.
[3] Kawabata Y, Tsuchida K, Imasaka T, Ishibashi N. Fiber-optic pH sensor with monolayer indicator. Analytical Sciences 1987;3:7–9.
[4] Jordan DM, Walt DR. Physiological pH fiber-optic chemical sensor based on energy transfer. Analytical Chemistry 1987;59:437–9.
[5] Werner T, Wolfbeis OS. Optical sensor for the pH 10–13 range using a new support material. Fresenius Journal of Analytical Chemistry 1993;346:564–8.
[6] http://probes.invitrogen.com/handbook/sections/2000.html.
[7] Cetinkaya B, Cetinkaya E, Brookhart M, White PS. Ruthenium(II) complexes with 2,6-pyridyl-diimine ligands: synthesis, characterization and catalytic activity in epoxidation reactions. Journal of Molecular Catalysis A: Chemical 1999;142(2):101–12.
[8] Ertekin K, Alp S, Karapire C, Yenigül B, Henden E, Icli S. Fluorescence emission studies of an azlactone derivative embedded in polymer films: an optical sensor for pH measurements. Journal of Photochemistry and Photobiology A: Chemistry 2000;137(2–3):155–61.
[9] Seiler K, Simon W. Theoretical aspects of bulk optode membranes. Analytica Chimica Acta 1992;266:73–87.
[10] Bakker E, Simon W. Selectivity of ion-sensitive bulk optodes. Analytical Chemistry 1992;64:1805–12.
[11] Lerchi M, Bakker E, Rusterholz B, Simon W. Lead-selective bulk optodes based on neutral ionophores with subnanomolar detection limits. Analytical Chemistry 1992;64:1534–40.
[12] Williams ATR, Winfield SA, Miller JN. Relative fluorescence quantum yields using a computer controlled fluorescence spectrometer. Analyst 1983;108:1067–71.
[13] Papkovsky DB, Ponomarev GV, Wolfbeis OS. Protonation of porphyrins in liquid PVC membranes: effects of anionic additives and application to pH-sensing. Journal of Photochemistry and Photobiology A: Chemistry 1997;104:151–8.
[14] Lobnik A, Oehme I, Murkovic I, Wolfbeis OS. pH optical sensors based on sol–gels: chemical doping versus covalent immobilization. Analytica Chimica Acta 1998;367(1–3):159–65.